Nano Energy 101 (2022) 107567

Contents lists available at ScienceDirect

Nano Energy

journal homepage: www.elsevier.com/locate/nanoen

Boosting the lifespan of magneto-mechano-electric generator *via* vertical installation for sustainable powering of Internet of Things sensor

Min Sub Kwak [a,1], Mahesh Peddigari [a,b,1], Yuho Min [a,c], Jong-Jin Choi [a], Jong-Hyun Kim [d], Michael Abraham Listyawan [e], Jungho Ryu [e], Geon-Tae Hwang [a,f], Woon-Ha Yoon [a], Jongmoon Jang [a,*]

[a] Department of Functional Ceramics, Korea Institute of Materials Science (KIMS), Changwon 51508, Republic of Korea
[b] Department of Physics, Indian Institute of Technology Hyderabad, Kandi, Telangana 502284, India
[c] School of Materials Science and Engineering, Kyungpook National University, Daegu 41566, Republic of Korea
[d] Korea Electrotechnology Research Institute (KERI), Changwon 51543, Republic of Korea
[e] School of Materials Science and Engineering, Yeungnam University, Gyeongsan 38541, Republic of Korea
[f] Department of Materials Science and Engineering, Pukyong National University, Busan 43241, Republic of Korea

ARTICLE INFO

Keywords:
Magneto-mechano-electric energy harvester
Single-crystal macro fiber composite
Accelerated life test
Lifetime
Reliability

ABSTRACT

Sustainability is essential for magneto-mechano-electric (MME) energy harvesters that convert low-frequency magnetic noise into useful electrical energy to be considered a practical power source for implementing real-life Internet of Things (IoT) sensor networks. In this study, we propose a vertically installed MME energy harvester based on a piezoelectric lead magnesium niobate-lead zirconate titanate ($Pb(Mn_{1/3}Nb_{2/3})O_3$-Pb(Zr,Ti)O_3, PMN-PZT) single-crystal macro fiber composite cantilever. The MME harvester generates 12.2 mW output power from a low-amplitude stray magnetic field of 2.5 Oe and exhibits a long-term usable lifetime of 2.5×10^9 cycles while maintaining over 90 % of its output. An accelerated life test method is employed to predict the usable lifetime of the MME harvester using an inverse power law-Weibull model with accelerating stress of magneto-mechanical vibration-induced strain. In addition, a standalone wireless environmental monitoring system is demonstrated to operate for 10 weeks by exploiting the harvested power from stray magnetic fields (~2.2 Oe) near the power cables of home appliances. This study paves the way for lifetime assessment and prediction of sustainable MME harvesters to increase the practicability of self-powered IoT devices in smart infrastructures.

1. Introduction

The emergence of the industry 4.0 revolution has led to the development of Internet of Things (IoT) based smart infrastructures to enable the communication between various interconnected devices, collect/access the data in remote control, monitor/manipulate the operations, provide a direct interface between users and their environment, and reduce human intervention [1,2]. The practical implementation of the IoT paradigm requires the proliferation of wireless sensor networks (WSNs) in infrastructures, which necessitated the utilization of standalone power sources that dealt with the limitations of conventional power sources (*i.e.*, batteries and capacitors) such as maintenance, accessibility, and limited lifespan [3]. In this context, energy harvesting technology (EHT) is widely adopted to design self-powered wireless sensor systems [4–6] for the next generation IoT devices by harvesting electrical energy from the surrounding environment such as mechanical [7–9], thermal [10,11], solar [12,13], and stray magnetic fields [14–23]. Among them, low-frequency (*e.g.*, 50 or 60 Hz) stray magnetic fields with amplitudes below 1 mT are ubiquitous around the current-carrying cables of the infrastructures where WSNs would be deployed. Thus, stray magnetic fields have emerged as promising harvestable energy sources for powering IoT devices.

The magneto-mechano-electric (MME) energy harvesting method that utilizes the magneto-mechanical torque as an excitation source to produce high power from low-frequency stray magnetic fields has drawn considerable attention for developing self-powered IoT systems [22,24].

* Corresponding author.
E-mail address: jongmoon@kims.re.kr (J. Jang).
[1] These authors contributed equally to this work.

https://doi.org/10.1016/j.nanoen.2022.107567
Received 11 April 2022; Received in revised form 19 June 2022; Accepted 30 June 2022
Available online 3 July 2022

In general, an MME harvester consists of a resonating cantilever structure with an attached magnetic proof mass, an elastic layer, and piezoelectric layers. The MME harvester converts the magnetic noise field into useful electric energy *via* two important mechanisms: (a) conversion from the magnetic field into mechanical vibration by the magneto-mechanical torque effect and (b) conversion from the mechanical vibration to electric field generation through the direct piezoelectric effect [17]. The concept of MME harvesters to harvest mechanical, as well as magnetic energy at low frequency (20 Hz), was proposed by Dong et al. in 2008 [25]. Later, various strategies have been employed to enhance the output performance of MME harvesters by utilizing low-loss anisotropic piezoelectric single-crystal fibers [15,20,22], and high-performance magnetostrictive materials (by replacing the elastic layer) [17,26] and adopting advanced structural engineering approaches such as magnetic flux concentration [18], distributed magnetic torque [23], multilayered ME composites [19], and triboelectrification [16].

In addition to generating sufficient output power in an MME harvester, it is essential to perform a reliability investigation to ensure a sufficient lifetime of the device for practical implementation. Although considerable progress has been made to enhance the output power of MME harvesters, it is rare to simultaneously present high output and long lifespan because sustaining a longer life while maintaining high output power is challenging owing to a trade-off between them. For example, Lim et al. [16] reported that adopting triboelectrification in MME generators using water-soluble nano-bullet modified nanostructures enabled a maximum output power generation of 4.8 mW at 7 Oe; however, it exhibited a shorter usable lifetime of 3.3×10^7 cycles. In other studies, Annapureddy et al. [20] demonstrated that using a low-loss lead magnesium niobate-lead zirconate titanate (PMN-PZT) single crystal-based piezoelectric material dramatically increased the output power of a magnetoelectric (ME) coupled MME harvester and displayed a rather low but stable output power of 40 nW (corresponding power density of 115 nW/cm^3) over 10^8 resonance fatigue cycles without any significant degradation. Lee et al. reported a novel strategy to generate high-power (~6.3 mW) from low amplitude stray magnetic fields (< 5 Oe) using a multilayer ME coupled MME harvester; however, the reliability of the MME harvester was not performed [19]. Moreover, although the actual lifetime of an MME harvester is very long, performing the reliability measurement until failure occurs is a time-consuming and costly process, and a methodology of evaluating and predicting the reliability of an MME harvester is yet to be established. In our previous study, the lifespan of a vibration-based piezoelectric energy harvester has been evaluated by an accelerated life test (ALT) using temperature as accelerated stress [8]. Therefore, the ALT can be applied to predict the power sustainability and lifetime characteristics of MME harvesters at low-amplitude stray magnetic fields. In addition, studies that can provide reliability investigations and practical demonstrations using stray magnetic fields, which are crucial for successfully deploying MME harvesters as sustainable power sources in IoT applications, are yet to be conducted.

In this study, we demonstrated a vertically installed MME (VI-MME) harvester constructed using a d_{32} mode Mn-PMN-PZT single-crystal macro fiber composite (SFC), a Ti cantilever structure, and a NdFeB magnetic proof mass that can generate a high output power exceeding 10 mW power with an outstanding usable lifetime of 2.5×10^9 at a practically available magnetic field of 2.5 Oe. The usable lifetime of the MME harvester in a normal use condition (~2.5 Oe) was estimated by applying an ALT method using the magnetic field-induced mechanical strain as accelerated stress. Further, a standalone wireless sensor system was demonstrated using the MME harvester to monitor temperature and humidity information in real time by harvesting the stray magnetic fields around the power cable of home appliances for 10 weeks.

2. Materials and methods

2.1. Fabrication of the MME harvester

For the fabrication of the MME harvester, solid-state grown d_{32} mode undoped and 1 mol% Mn-doped PMN-PZT single crystal-based macro fiber composites (SFCs) (Ceracomp Co. Ltd, Korea) are used as piezoelectric layers. The PMN-PZT piezo-fibers are aligned within an epoxy matrix [28 (l) × 14 (b) × 0.2 (t) mm^3] and symmetrically sandwiched between 100-nm thick gold (Au) electrodes, 18-μm-thick copper (Cu) electrical lines, and polyimide encapsulation [42 (l) × 21 (b) × 0.5 (t) mm^3]. The detailed fabrication procedure of the SFCs is provided in our previous study [27,28]. Flexible titanium alloy (grade 5) cantilevers having the dimensions of 100 (l) × 20 (b) × 0.3 (t) mm^3 are used as elastic layers and bonded to the SFCs by using a structural epoxy adhesive (DP-460, 3 M). Thin electrical wires are connected to the electrode pads *via* soldering to measure the output voltage from the SFCs. NdFeB alloy magnets (N35 grade) with a total weight of 34 g are attached at the end of the cantilever structure to serve as a magnetic proof mass to form an MME generator.

2.2. Simulations

Finite element analysis (FEA) modeling was performed using the COMSOL Multiphysics program (Ver. 5.3) to simulate the gravity effect on the strain applied to the MME harvester. A geometrical cantilever structure consisting of a piezoelectric layer (28(l) mm × 0.2(t) mm) covered with Kapton layers (0.05(t) mm) and attached to a grade-5 Ti substrate (100(l) mm × 0.3(t) mm) was used for performing the FEA. To adjust the resonance frequency of the structure to 60 Hz, two N35 magnets (10(l) × 12.53(t) mm) were placed at the end of the cantilever. The electrical and mechanical properties of the materials applied for structure analysis are provided in Table S1 and S2, Supporting Information**.** To simulate the horizontal MME configuration, the cantilever with the piezoelectric layer end was fixed and applied the downward force perpendicular to the body ($F = -\rho g$, where ρ is density and g is gravitational acceleration) for mimicking the gravity force, as shown in Fig. S1. The alternating vibration force generated by an external magnetic field was applied to the N35 magnets to realize dynamic vibration.

2.3. Characterization

A Helmholtz coil (M-MHC125, MMS company, Korea) with a coil factor of 6 Oe/A, equipped with a high-speed bipolar amplifier (HSA 4051, NF corp., Japan) and a function generator (WF1948, NF corp., Japan), was used to produce a uniform magnetic field. To apply the magnetic fields homogeneously, the MME generators were placed at the center point along the axis of the Helmholtz coil. The applied magnetic field on the MME generator was controlled by the current passing through the Helmholtz coil and further confirmed using a Gauss meter. To measure the applied strain on the SFC under the influence of the applied magnetic field, a strain gauge (MFLA-5–350–11–1LS, Tokyo Sokki Kenkyujo Co., Ltd, Japan) with a 350 Ω resistance was attached on the top surface of the SFC with an M-bond 200 adhesive, and the resistance change under a cyclic mechanical force was measured using a digital data acquisition (DAQ) (USB-2404-UI, Measurement Computing corp., USA) interfaced computer system. A digital oscilloscope (Wave surfer 44Xs-A, Lecroy corp., USA) was used to record time-dependent output voltage waveforms. The output power from the MME harvester is rectified and regulated using an LTC 3588 power management IC (Linear Technology corp., USA). To demonstrate the powering of real-life IoT applications, an integrated wireless sensor communication system (LYWSD03MMC, Xiaomi Inc., China) and a smartphone (Galaxy S20 Ultra, Samsung Electronics Co. Ltd., Korea) were used.

3. Results and Discussion

3.1. Vertically installed MME generators with high output power and longer lifetime operation at a low-amplitude stray magnetic field

For efficient power generation from ubiquitous stray magnetic fields arising from electrical power lines, we propose a novel approach with a robust MME harvester. Fig. 1a schematically illustrates the basic operation of the proposed MME harvester and the overall concept of this work. The MME harvester is designed to operate vertically suspended to utilize a longer cantilever structure and a heavier magnetic proof mass as illustrated in Fig. 1a. The insets in Fig. 1a further illustrate the schematics of exceeding 10 mW (1.01 mW/cm^3. Oe) power generation from 60-Hz low-amplitude stray magnetic fields (Fig. 1a-i), the reliability estimation for the MME generator using statistical failure data obtained *via* the ALT method (Fig. 1a-ii), and the practical demonstration of powering WSN systems using stray magnetic fields generated from the electrical power line of home appliances (Fig. 1a-iii).

The MME generator fabricated using a d_{32} mode configured 1 mol% Mn-doped PMN-PZT based single-crystal macro fiber composite (SFC; 28 (l) × 14(w) × 0.2(t) mm^3) (Ceracomp Co. Ltd, Korea) as a piezo component, a cantilever structured flexible non-magnetic grade-5 Ti sheet (100(l) × 20(w) × 0.3(t) mm^3) with low mechanical loss and high elastic modulus (~114 GPa) as an elastic layer, and strong NdFeB permanent magnets (grade N35, 34 g) as proof masses. The SFC and Ti elastic layers were laminated using a structural epoxy adhesive (DP 460) and rigidly clamped using a Bakelite zig, while the magnetic proof mass was attached at the other end of the cantilever as shown in Fig. 1b. The inset of Fig. 1b reflects the flexibility of the SFC and high compliance, which is essential for driving harsh low-frequency bending motions and sustaining high strain magnitudes. The schematic of the exploded view of the SFC is shown in Fig. 1c. The SFC with <011> -d_{32} crystallographic orientated single crystal fibers was adapted owing to its high-power generation ability than other configurations (<001>-d_{31} and <011>-d_{31}) under identical loading conditions [22]. Since the figure of merit (FOM), *i.e.*, the product of electromechanical coupling factor (k_{ij}) and mechanical quality factor (Q_m) of the piezoelectric single crystals is an important factor to realize the high-power efficiency, the 1 mol% Mn-doped PMN-PZT single crystal fibers were used in this study. The 1 mol% Mn-doping significantly reduced the spontaneous polarization and caused the internal bias field as evidenced from the polarization–-electric field (*P-E*) loops (Fig. 1d), thus inducing the hardening behavior in the PMN-PZT single crystals. This behavior is ascribed to the creation of oxygen vacancies (inset of Fig. 1d) by doping with the acceptor ions (such as $Mn^{3+,2+}$) in the B-site of ABO_3 perovskite piezoelectric ceramics, which assists clamping the domain wall motion and restricts the spontaneous polarization and thus inducing the hardening behavior [29]. In addition, the Q_m estimated from the impedance spectra using the −3 dB bandwidth method (= $f_r/\Delta f$) showed a 334 % improvement with 1 mol% Mn-doping (Fig. 1e), which resulted in the enhanced FOM of the PMN-PZT single crystals and thus output performance of MME harvesters (Fig. S2). The inset of Fig. 1e shows the photographs of the PMN-PZT single crystals that were used to measure the material properties. The detailed electromechanical properties of the SFCs and mechanical properties of MME harvester are detailed in Tables S1-S2.

In general, the MME generator's output performance mainly depends on the magneto-mechano vibration from the excitation force and the applied stress magnitude on the piezoelectric phase [17–19]. Previous research suggested that the magnetic proof mass volume (or weight) determines the magneto-mechano vibration amplitude and the resonance frequency of an MME harvester [19]. For the bending vibration in the cantilever beam, the force exerted on the cantilever due to the magneto-mechano torque ($\tau = (M \times B)$. V) of the magnetic proof mass generated under the external magnetic field (B) (schematically shown in Fig. S3) is proportional to the magnetization (remnant flux density) and the volume of the magnetic proof mass. Therefore, adding a heavy magnetic proof mass can generate higher magnetic torque and increase the vibration amplitude of the cantilever beam, which leads to an enhanced output power even under low-amplitude alternating current (AC) magnetic fields. However, the addition of heavy proof mass to realize high output power from the MME harvester in the fundamental flexural mode will have the consequences of (1) larger shift in the resonance frequency from the desired frequency of 50/60 Hz and (2) early failure of MME harvester due to the large tip displacement. In this scenario, utilization of the 2nd harmonic resonance mode allows the addition of heavier magnetic proof mass, thereby enhancing the power efficiency of the MME harvesters [16,30]. Fig. 2a shows the COMSOL Multiphysics simulation for the vibration displacement profile of the MME harvester under 2nd harmonic resonance condition. As can be seen from the Fig. 2a and Fig. S2b, the maximum displacement is appeared around the center of the cantilever beam, which can apply relatively larger stress on the piezoelectric phase despite the smaller tip displacement amplitude, thus enhancing the power efficiency. Therefore, we adopted the 2nd harmonic resonance mode for the MME harvester in this study. However, the heavy magnetic proof mass at the end of the cantilever causes initial bending due to the gravitational force (Fig. 2b and Fig. S1), and its effect is theoretically simulated by finite element analysis (FEA) using the COMSOL Multiphysics as shown in Fig. 2c and Fig. S1. The mechanical strain applied to the SFC is simulated for the gravity-affected MME harvester (i) and the non-gravity MME harvester (ii) under the vibration *via* magnetic-mechano torque. Fig. 2d shows that the magnitude of the simulated strain is similar in both conditions ($\varepsilon_{peak\ to\ peak} \approx 2190$ με with gravity and 2180 με without gravity); however, a significant pre-strain (~1570 με) is identified at the MME harvester model under the influence of gravity. To minimize the effect of the downward stress of the SFC due to gravity on the durability of the device, we proposed to install the MME harvester in a vertical direction. To analyze the applied stress on the SFC, we experimentally measured the applied strain on the SFC using strain gauges (Fig. S4) by mounting the MME harvester in horizontal and vertical directions under a 2.5 Oe magnetic field at the resonance condition (60 Hz). The MME harvesters exhibited similar peak-to-peak strains installed in the vertical (~2480 με) and horizontal (~2680 με) configurations. The vertically installed MME harvesters did not show significant pre-strain compared to when installed horizontally (~1450 με). In addition, the generated output voltage waveform with the horizontal configuration shows an asymmetric voltage waveform and exhibited a slightly higher root mean square power (P_{rms}) than that with the vertical configuration (Fig. 2e and Fig. S5, Supporting Information). Here, the P_{rms} (= V_{rms}^2/R_L) of the harvesters was estimated by measuring the output voltage (V_{rms}) at various load resistances (R_L) from 1 kΩ to 1 MΩ. We also investigated the fatigue behavior of the MME harvester in both configurations by measuring its life cycles at the resonance frequency (60 Hz) with an optimized load resistance condition as shown in Fig. 2f. The obtained fatigue results indicated that the vertical installation effectively reduced the gravity-induced stress on the SFCs as well as changes in the resonance frequency, thereby enhancing the lifetime of the MME harvesters. Therefore, the proposed vertical configuration can fabricate reliable MME harvesters with longer lifetimes and efficiently harvest the power from low-amplitude 50/60 Hz AC magnetic fields. Further, we optimized the cantilever length (~10 cm) and the required tip mass (~34 g) at the end of the cantilever (Fig. S6) to generate a sufficient output power (> 10 mW) from the MME harvester to realize the self-powered WSNs in a low magnetic field of 2.5 Oe at 60 Hz [24,31].

3.2. Lifetime prediction of the vertically installed MME harvester using accelerated life test (ALT) method

Assessing the reliability of the VI-MME harvesters in terms of fatigue evaluation or usable lifetime estimation is necessary for their deployment in practical applications. However, the VI-MME harvester has demonstrated an excellent fatigue endurance up to 10^8 cycles, and

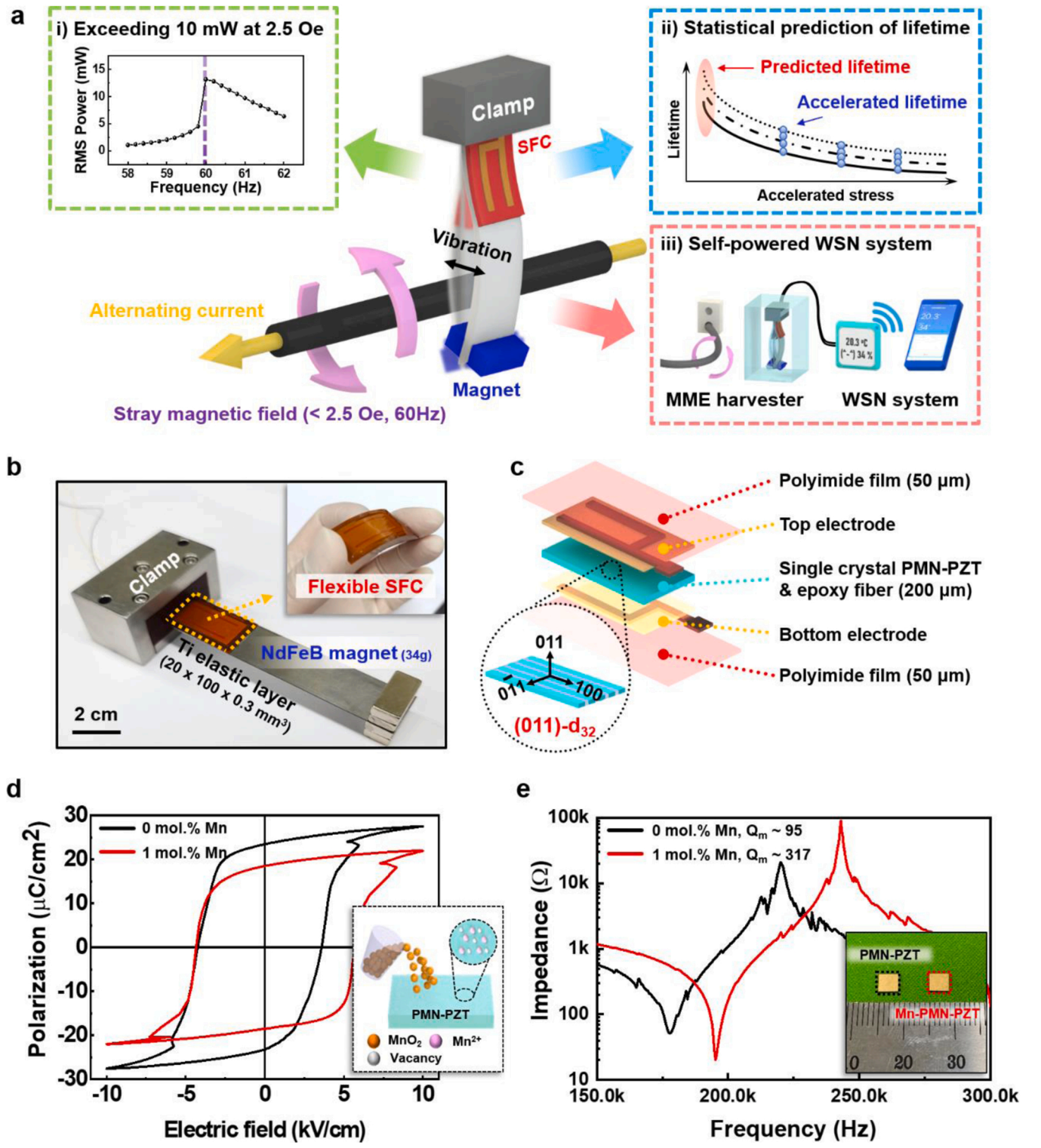

Fig. 1. *Overall concept of VI-MME harvester* (a) Schematic illustration describing the working mechanism and structural design of magneto-mechano-electric (MME) energy harvester to produce high power from the low-amplitude magnetic noise around the electric power cables. Schematic illustrations showing the i) high power generation at resonance condition by scavenging the low-amplitude 60 Hz stray magnetic fields, ii) statistical prediction of lifetime using accelerated life test method, and iii) demonstration of self-powered wireless sensor network system. (b) Photograph of the fabricated MME harvester, showing the SFC and permanent magnets bonded to Ti elastic layer. (c) Schematic showing the exploded view of the SFC and crystallographic orientation of single crystal macro fibers. (d) Polarization-electric field hysteresis loops and (e) impedance spectra of the undoped and 1 mol% Mn-doped PMN-PZT single crystals. The insets of (d) and (e) represents the Mn-doping induced hardening behavior in PMN-PZT single crystals and the photograph of the used single crystals, respectively.

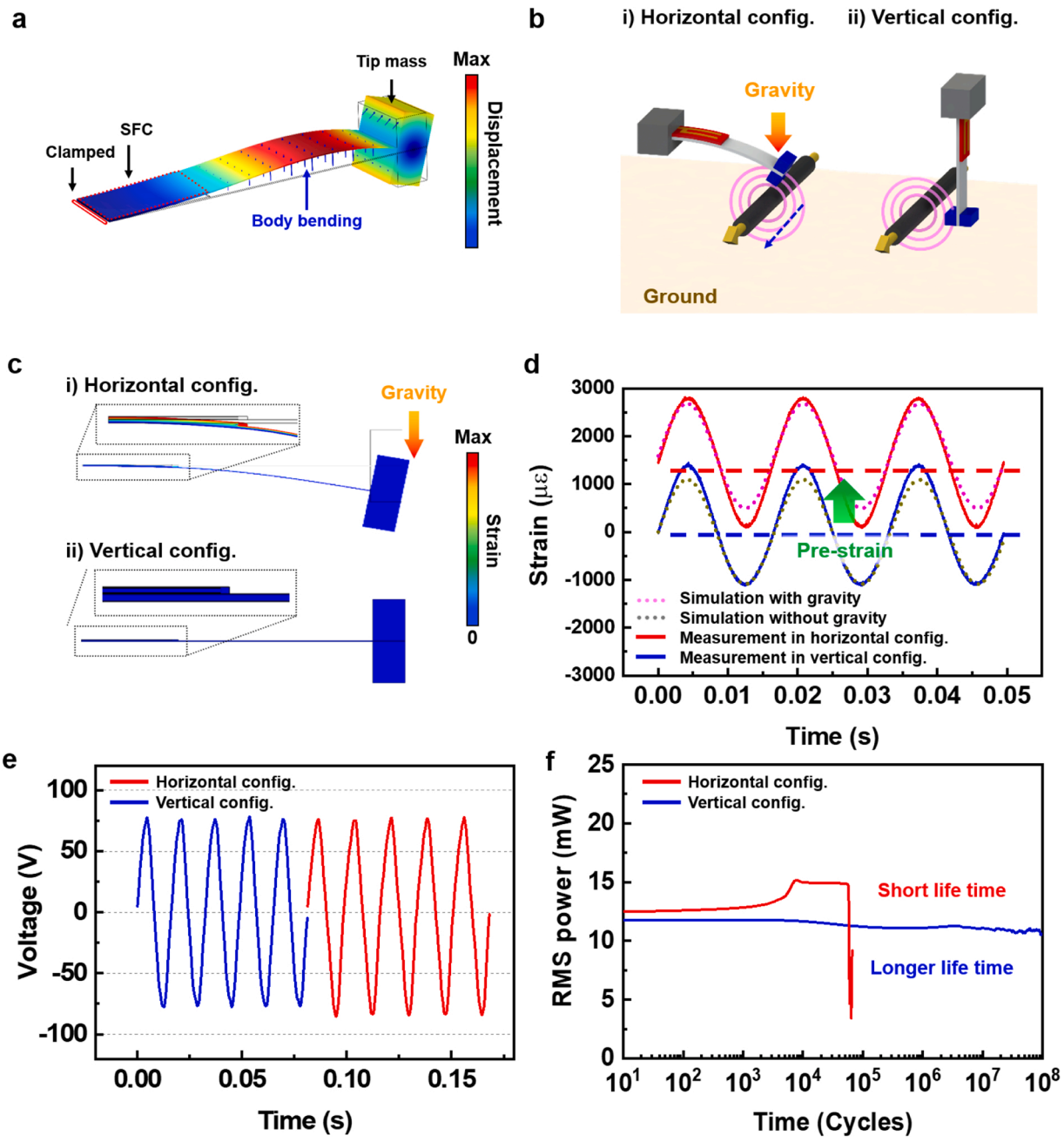

Fig. 2. *Output performance of VI-MME harvester* (a) The FEA simulated vibration displacement profile of the MME harvester in the 2nd harmonic bending resonance mode. (b) Schematic representations and (c) FEA simulation results for strain distribution of the MME harvesters operating under the influence of (i) gravity and (ii) without gravity. (d) Comparison of strain results obtained theoretically and experimentally for the MME harvesters configured in horizontal and vertical directions. Comparison of (e) open-circuit voltage waveforms and (f) working life (or fatigue behavior) of the MME harvesters operated in horizontal and vertical configurations.

further evaluation until failure occurs in the harvester is a time-consuming and costly process. Therefore, the ALT method is essential to determine the reliability of the VI-MME harvesters. It provides a feasible way to assess the reliability of a specimen under normal use conditions in an affordable time by conducting the measurement at higher stress conditions, such as elevated temperature, mechanical stress, electric/magnetic field, humidity, and vibration. Also, the statistically acquired time-to-failure data are applied to an appropriate stress-response lifetime regression model to extrapolate to normal conditions [32].

In this regard, a quantitative accelerated test Type B was applied based on international standards (IEC 62506:2013) [33], which estimates the expected life of the specimen by inducing a significant cumulative damage in a shorter time than the predicted life. The detailed procedure for applying the ALT is provided in our previous study [8], which involves (1) design of the test (identification of potential failure modes/mechanisms and selection of accelerating stress, accelerating stress levels, test duration, and number of testing samples), (2) progress of the test (performance of experimental run-test based on defined failure criteria), (3) reliability analysis (estimation of usable lifetime in the normal use condition using time-to-failure distributions and life-stress relations), and (4) failure analysis.

Since most of the physical and chemical processes involving MME harvester failures such as delamination, cracks, and fatigue behavior of the components depend on the applied magnetic field-driven mechanical stress, the magnetic field was chosen as the accelerated stress to

induce/accelerate the failure mechanisms in the VI-MME harvester [34]. The fatigue behavior of MME harvesters can be more severe under high magnetic field environments than the normal magnetic noise around the power cables. Therefore, a quick failure data at high magnetic field stress levels yields information on the lifetime distributions and allow the lifetime estimation of the MME harvesters under normal use conditions.

The purpose of designing and fabricating the proposed high-performance MME harvesters is to harvest useful electrical energy from ambient stray magnetic fields to power wireless sensor network systems. Although it varies from country to country, in general, the amplitude of stray magnetic fields in household environments lies up to 3 Oe with a frequency of 50/60 Hz near the electric devices; especially near high joule heating generators, such as air conditioners, space heaters, and hairdryers [19]. For example, in the main electricity environment of 220 V and 60 Hz, a current-carrying cable of an air conditioner generates a magnetic noise of approximately 2.5 Oe at a distance of 5 mm (Fig. S7). Therefore, we attempted to investigate the output performance of the proposed MME harvester by applying a 60 Hz magnetic field of 2.5 Oe using a Helmholtz coil. Under this applied magnetic field, the SFC experienced a maximum strain of 1300 με (Fig. 3a), and the MME harvester generated a P_{rms} of 12.2 mW (corresponding power density is 1.01 mW/cm^3. Oe) at an optimum load resistance of 80 kΩ (Fig. 3b). Here, the power density of the VI-MME harvester is estimated by including the volumes of piezoelectric layer, elastic layer, and magnetic proof mass. The obtained output power density from this VI-MME harvester is much larger than that of the state-of-the-art of the ME coupled MME harvesters as listed in Table 1. Herein, the enhanced output performance is attributed to the adequate structural design with the addition of the heavy magnetic proof mass, which significantly amplified the magneto-mechano vibration and stress applied to the piezoelectric SFC, thereby achieving an enhanced output

Table 1
Output power density comparison of the state-of-the-art MME harvesters.

MME harvester structure	Power density [mW/cm^3.Oe]	Ref.
PMN-PZT SFC / Fe-Ga	0.46	[12]
Piezoelectric MFC / Metglas	0.208	[14]
PZT-5A / Metglas	0.31	[16]
Low-loss PMN-PZT SFC / Ni	0.3	[17]
VI-MME PMN-PZT SFC / Ti	1.01	This work

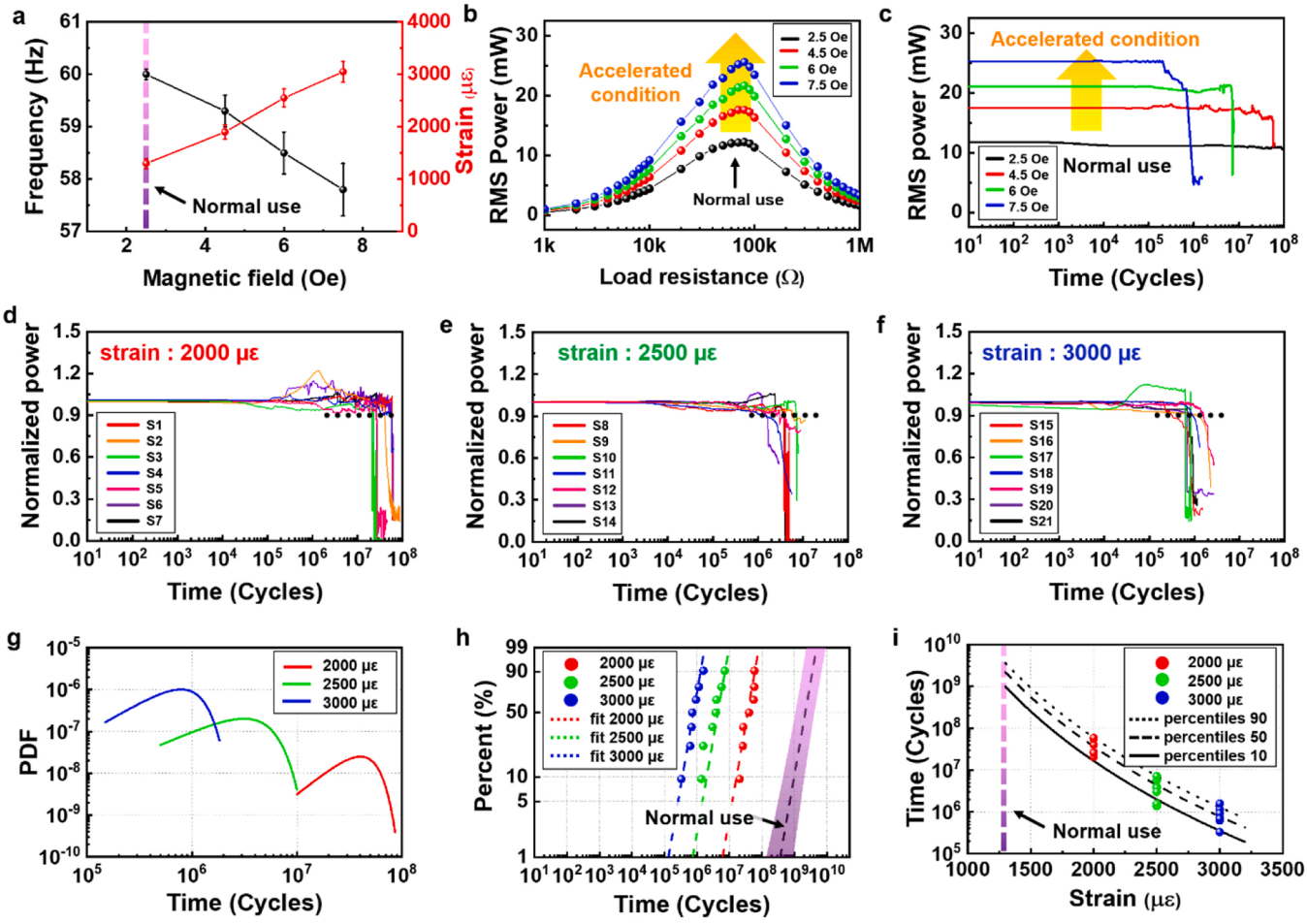

Fig. 3. *Lifetime estimation of VI-MME harvester using ALT method* (a) Measured resonance frequencies of the VI-MME harvester and applied mechanical strain on the SFC as a function of magnetic field strengths. The generated RMS output power (P_{rms}) from the VI-MME harvesters as a function of (b) load resistances, and (c) fatigue cycles measured at normal use (2.5 Oe) and accelerated stress conditions (4.5, 6, and 7.5 Oe). Normalized output power of the VI-MME harvesters as a function of fatigue cycles measured at the accelerated stress conditions of (d) 2000 με, (e) 2500 με, and (f) 3000 με. Seven different samples (S stands for sample) are used at each stress condition to obtain statistical values of the lifetime. The black color dotted line indicates the 10 % power reduction level. (g) The probability density function of Weibull distribution of the obtained statistical failure data of the VI-MME harvesters. (h) The inverse power law–Weibull (I-W) model fitting curves to predict the usable lifetime of the VI-MME harvesters at the normal use condition (1300 με) by using a maximum likelihood estimated shape parameter of 2.38. The purple-shaded area represents the 95 % confidence interval. (i) The extrapolated life-stress curves to estimate the lifetimes of VI-MME harvester at the normal use condition with different failure percentiles.

power even from weak magnetic fields. For instance, we fabricated the VI-MME harvesters with different polycrystalline piezoelectric ceramics and measured their output performance under identical excitation conditions to accentuate the significance of the proposed harvester's design. Although the power density of polycrystalline ceramic-based VI-MME harvesters (0.3–0.35 mW/cm^3. Oe) is almost three times less than the SFC-based VI-MME harvester (Fig. S8), they still exhibited higher power density than the ME coupled MME harvesters (Table 1). Moreover, it is interesting to note that the VI-MME harvester generated a highly stable output power over 10^8-fatigue cycles (Fig. 2f) without any significant degradation, demonstrating the durability of the proposed harvester.

In this study, the magnetic field of 2.5 Oe is considered as the normal use condition because most of the household current-carrying cables can generate the maximum magnetic noise in the range of 2–3 Oe. Therefore, we perform the ALT at three different magnetic field environments of 4.5 Oe, 6 Oe, and 7.5 Oe using the Helmholtz coil under identical measurement conditions such as identical clamping, weight, and position of the magnetic proof mass to avoid other artifacts. We chose these accelerated stress levels to satisfy the conditions of international standards for ALT type B, such as the accelerating stress should not be so large as to cause the unexpected damage that would not occur under normal operating conditions, and the experiment should not take longer times under the accelerated stress conditions. A bipolar amplifier equipped with a function generator is used to control the magnetic field produced by the Helmholtz coil. To record the usable lifetime of each VI-MME harvester, the output power of the harvesters is continuously monitored (until failure occurs) during the tests. The ALT experiment is performed with seven samples at each accelerated stress condition for better repeatability of the measured lifetime.

To quantify the applied magnetic field-induced mechanical stress on the VI-MME harvesters, we measure the mechanical bending strain experienced by the piezoelectric SFCs under various magnetic field environments using the strain gauge method and provided the estimated maximum strain values as a function of the applied magnetic field strength in Fig. 3a. The measured maximum strain amplitudes at 2.5, 4.5, 6.0, and 7.5 Oe magnetic fields are 1300 ± 100, 1900 ± 140, 2550 ± 170, and 3050 ± 200 με, respectively. Similar to the magnetic field-induced mechanical strain, the generated output P_{rms} also exhibited a linear relation with the applied magnetic field as shown in Fig. 3b. The corresponding sinusoidal voltage waveforms measured under optimized load resistance conditions are shown in Fig. S9. The peak P_{rms} is progressively increased by increasing the accelerating stress as 17.6, 21.7, and 25.6 mW generated under 4.5, 6.0, and 7.5 Oe magnetic fields, respectively, whereas the resonance frequency decreased from 60 Hz to 57.8 Hz as evidenced in Fig. 3a-b. This is because of the amplified magneto-mechanical torque-induced enhanced bending moment (or mechanical stress) of the MME harvester under high magnetic field environments. Fig. 3c depicts the comparison of the fatigue behavior of the VI-MME harvesters measured at various magnetic field stress conditions. Notably, a significant decrease in a usable lifetime is noticed with an increase in the accelerated stress intensity, which indicates that the magnetic field (strength) can be used as accelerated stress to accelerates the life of the VI-MME harvesters.

Since the relationship between the accelerated stress and the induced mechanical strain is established, the fatigue evaluation of the VI-MME harvesters is performed at the accelerated stress conditions by subjecting them to the strain values of 2000, 2500, and 3000 με. In this study, the VI-MME harvesters are considered as failed when one of these events occurs: (1) 10 % reduction in the output power and (2) functional failure in the sample [35–37]. Fig. 3d–f show the variation in the normalized P_{rms} of the VI-MME harvesters as a function of the fatigue cycles measured at different stress conditions. Here, the normalization is done with respect to the initial P_{rms} value. The time-to-failure (TTF) of each VI-MME harvester used in this ALT is obtained based on the defined failure criteria, as seen in Table S3. The average TTFs of the VI-MME harvesters measured at 2000, 2500, and 3000 με strain levels are 4.11×10^7, 3.81×10^6, and 5.10×10^5 cycles, respectively. A detailed failure analysis has been conducted to identify the most vulnerable points that affect the lifetime of the VI-MME harvester under accelerated stress conditions, and the results are provided in Fig. S10. It revealed that the magneto-mechanical vibration-induced cracks on top Cu electrodes are attributed to the VI-MME harvester failure at high accelerated stress conditions. In addition, the reusability of the failed VI-MME harvester is demonstrated by using the repaired top Cu electrodes (Fig. S11).

To analyze the distribution of the TTFs at various stress levels and assess the reliability in the normal use condition, using a suitable probability distribution for the TTFs and establishing a life-stress relation that relates the life behavior to the stress levels are essential. Mathematical functions for analyzing the theoretical distribution of lifetimes of devices include exponential, lognormal, gamma, and chi-square distribution models [38]. In this study, a two parameter Weibull distribution function is utilized to describe the obtained ALT data and analyzed using a statistical software (Minitab 19, Minitab Inc., USA) as this method is versatile, flexible and generally works best with data sets with smaller sample sizes that contain a complete data [39]. The Weibull probability density function (PDF) for the distribution of the TTFs can be expressed by the following equation, and the fitting results are shown in Fig. 3g.

$$f(t) = \frac{\beta}{\eta}\left(\frac{t}{\eta}\right)^{\beta-1} exp\left[-\left(\frac{t}{\eta}\right)^{\beta}\right],\ t \geq 0,\ \eta, \beta > 0, \tag{1}$$

where $f(t)$ is the failure probability density function, t is the usable lifetime (or TTF), η is the scale parameter or characteristic life (at which 63.2 % of the total samples fail), and β is the shape parameter. The distributions at each stress level are constructed with a two-sided 95 % confidence interval (*i.e.,* the probability of wrong fitting, $\alpha = 0.05$). Here, the parameter p, which represents the degree of reliability/accuracy of the test hypothesis, is found to be approximately 0.71 ($>>\alpha$). It indicates that the life of the VI-MME harvesters is accelerated by the applied mechanical strain. The estimated fitting parameters of η and β from the cumulative distribution curves (Fig. S12) by software are listed in Table 2.

Interestingly, the scale parameter shows an inverse relation with the applied accelerated stress. Therefore, the inverse power law (IPL) is employed to establish a mathematical relation between the applied mechanical strain (ε, accelerated stress) and the corresponding estimated characteristic lifetimes (η) [40].

$$\eta(\varepsilon) = \frac{1}{K\varepsilon^n}, \tag{2}$$

where $\eta(\varepsilon)$ represents a strain-dependent characteristic lifetime, and K and n are the model parameters to be determined. By combining the Weibull life distribution and IPL life-stress relation using the Eqs. (1) and (2) under the assumption of constant β for all accelerated stress conditions, the combined IPL-Weibull distribution can be written as below.

$$f(t, \varepsilon) = \beta K\varepsilon^n (K\varepsilon^n t)^{\beta-1} e^{-(K\varepsilon^n t)^{\beta}} \tag{3}$$

The maximum likelihood estimation (MLE) method has been utilized to estimate the IPL-Weibull parameters (β, K, and n) to fit the obtained ALT data well, and the obtained best-suited parameters are $\beta = 2.38$, ln

Table 2
The estimated Weibull distribution parameters of MME harvesters under different mechanical strain conditions.

Strain [με]	Scale parameter (η)	Shape parameter (β)
2000	4.60×10^7	2.98
2500	4.32×10^6	2.08
3000	9.75×10^5	2.44

(*K*) = − 89.6, and $n = 9.48$. In general, the shape parameter $\beta > 1$ represents an increase in the failure rate with the fatigue cycles, which is similar to the wear-out failure part of the well-known bathtub curve [37]. Fig. 3 h displays the probability of the failure (or unreliability) of the VI-MME harvesters as a function of the fatigue cycles at different stress levels. Notably, the experimentally obtained ALT statistical failure data are well-fitted (or reproduced) with the IPL-Weibull model using the MLE parameters. The Anderson-Darling values (represent the goodness of the fit) of 2.46, 1.81, and 2.22 are obtained for the stress levels of 2000, 2500, and 3000 με, respectively. Further, the probability of failure at the normal use condition (*i.e.,* 1300 με) with a 95 % confidence interval is estimated by extrapolating the ALT data with the

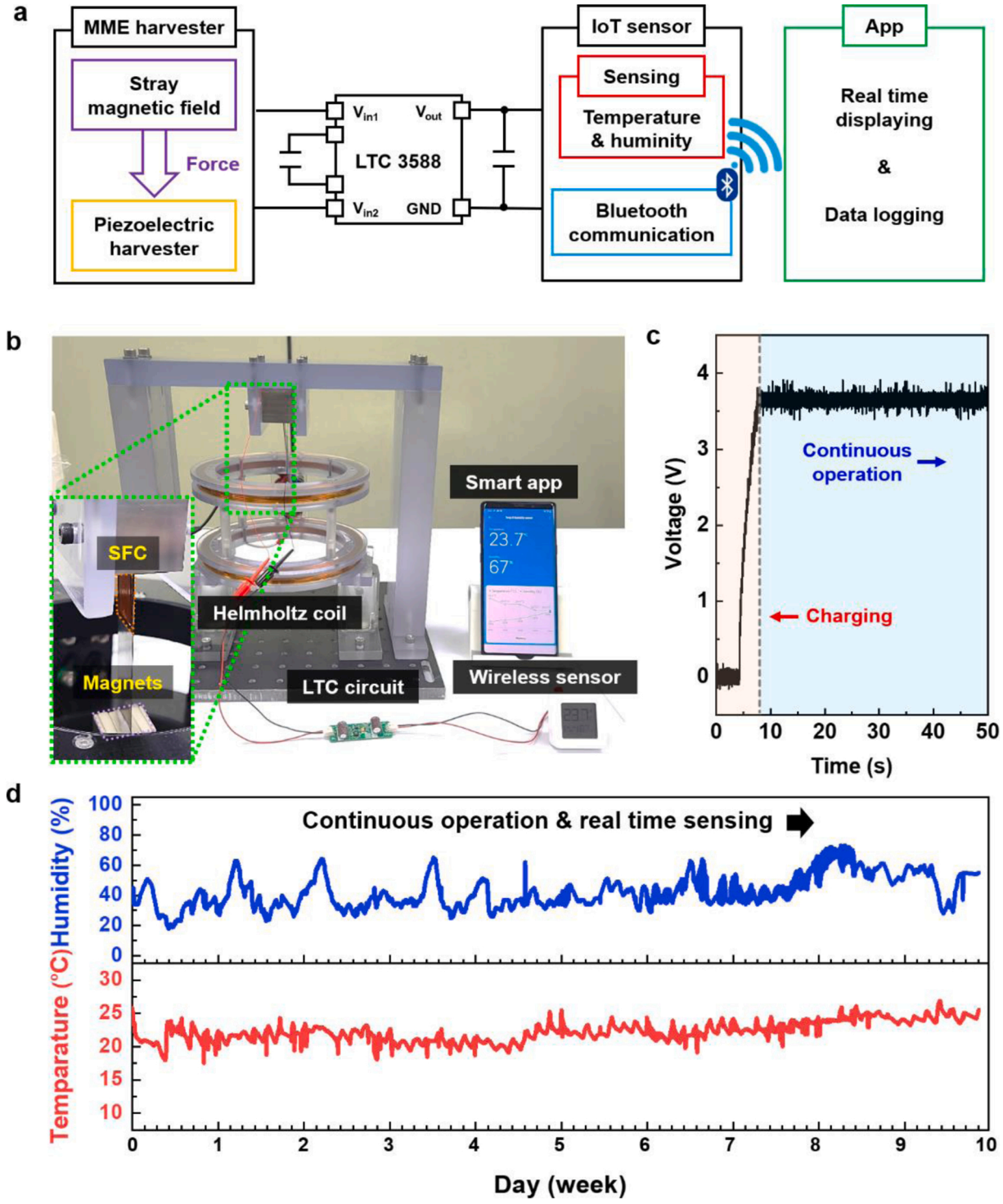

Fig. 4. *Demonstration of self-powered IoT sensor using the Helmholtz coil.* (a) Schematic circuit diagram of self-powered wireless sensor network system that comprising of VI-MME harvester, power management circuit, and wireless sensor module. (b) Photograph of the experimental setup used for demonstrating a self-powered wireless sensor system. (c) Charging-discharging characteristics of a 0.1 mF energy storage capacitor during the IoT sensor operation by using the energy generated from the VI-MME harvester. (d) The acquired temperature and humidity data for 10 weeks continuously from the IoT sensor powered by the VI-MME harvester using the magnetic field (2.5 Oe) produced by a Helmholtz coil.

IPL-Weibull model, as indicated by the black line with purple shaded area in the Fig. 3 h. The estimated average lifetime of the VI-MME harvester with a 62.3 % failure probability is approximately 2.5×10^9 cycles, which is equivalent to the continuous working life of 482 days at 60-Hz operation. The acceleration factors ($AF = (\varepsilon_a / \varepsilon_u)^n$) for the accelerated stress conditions of 2000, 2500, and 3000 με with respect to the normal use condition are found to be around 59, 492, and 2773, respectively, demonstrating the importance of ALT in reducing the time as well as cost for assessing the reliability of VI-MME harvesters. Here, ε_a and ε_u are the strain levels at the accelerated stress and normal use conditions, respectively. The estimated lifetimes of the VI-MME harvesters at different failure percentiles as a function of the applied strain are depicted in Fig. 3i. At the normal use condition, the predicted lifetimes of the VI-MME harvester with the failure percentiles of 10 %, 50

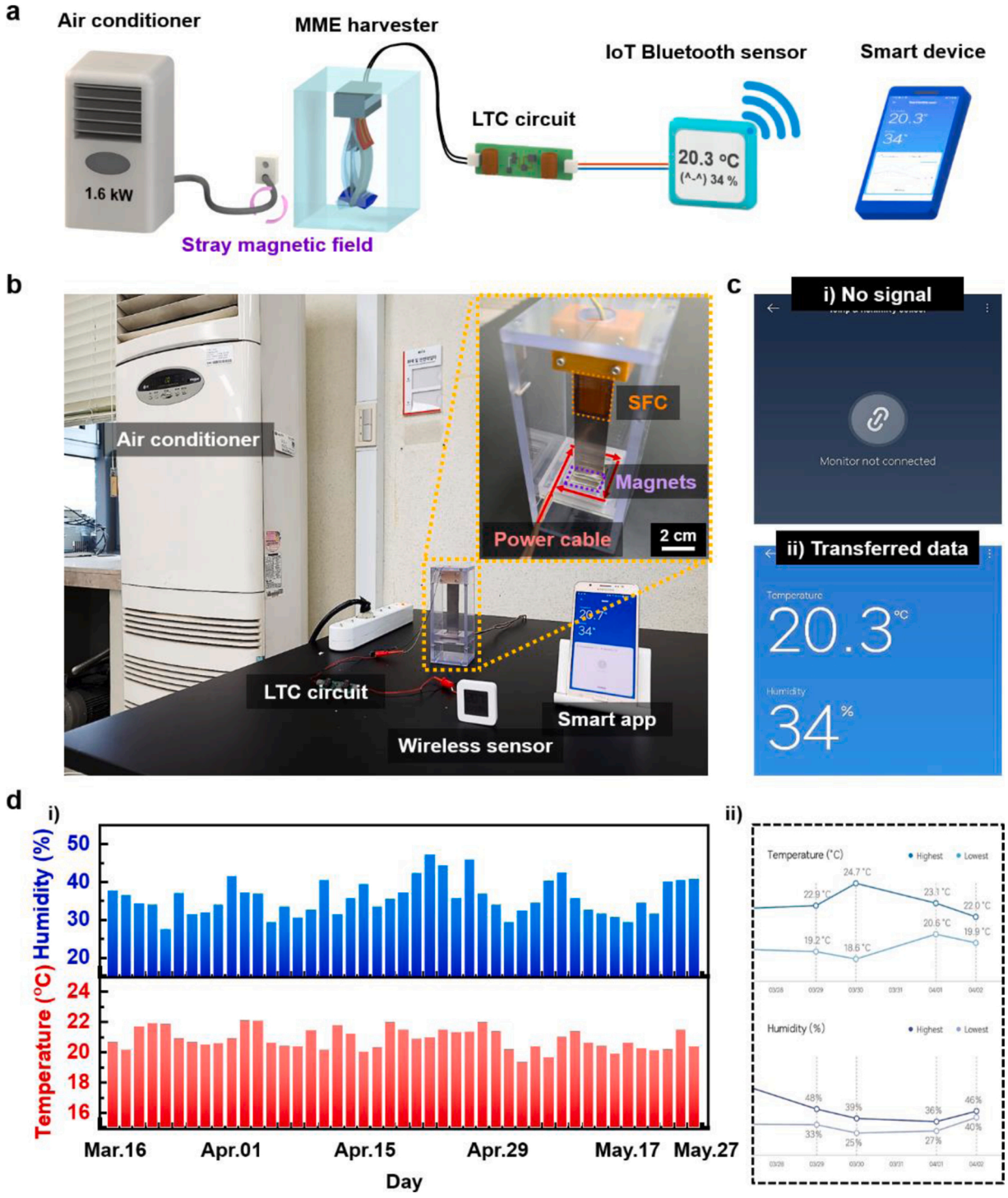

Fig. 5. *Demonstration of self-powered IoT sensor using the stray magnetic fields*. (a) Conceptual schematic of the working mechanism of Bluetooth-enabled self-powered wireless sensor system using the VI-MME harvester by scavenging the stray magnetic fields around the power cable of an air conditioner. (b) Photograph of the used experimental setup. (c) Captured images of the environmental (temperature and humidity) data monitoring application on a smartphone. (d) The sensed temperature and humidity data collected for 10 weeks from the Bluetooth-enabled self-powered IoT sensor system powered by VI-MME harvester, i) averaged daily data, and ii) the captured image of data logged in the monitoring application on a smartphone.

%, and 90 % are approximately 9.8×10^8, 2.2×10^9 and 3.6×10^9 vibration cycles, respectively. Therefore, the proposed VI-MME harvester having longer lifetime can serve as a sustainable power source for self-powered wireless sensor nodes.

3.3. Demonstration of self-powered IoT sensor using VI-MME harvester

To verify the feasibility of powering a wireless sensor system for longer durations using the power generated by the VI-MME harvester, we demonstrated continuous powering of a wireless environmental IoT sensor with a Bluetooth-based data transmission system for 10 weeks under the normal use condition (1300 με). Fig. 4a shows the schematic of the operation of a wireless sensor system. For this demonstration, a Helmholtz coil to produce the uniform magnetic field at 60 Hz, a commercially available LTC 3588 power management IC to rectify the output voltage from the VI-MME harvester and regulate the output power to drive the wireless IoT device (LYWSD03MMC, Xiaomi, China) that consisted of humidity and temperature sensors, and a smartphone to monitor the acquired sensing data *via* Bluetooth communication are used. Fig. 4b shows photograph of the assembled VI-MME harvester-powered IoT wireless sensor system. Fig. 4c depicts the charging and discharging profile of a 0.1 mF energy storage capacitor during the operation of the IoT wireless sensor system. Notably, the VI-MME harvester can charge the capacitor up to 3.6 V within approximately 4 s and power the IoT sensor module to sense as well as transmit the temperature and humidity information to the smartphone in real time *via* Bluetooth communication without any significant drop in the capacitor's voltage. The generated open-circuit voltage waveform under a uniform magnetic field (~2.5 Oe) produced by the Helmholtz coil is shown in Fig. S13. The power requirement for the IoT sensor during the wake-up and sensing states is estimated based on the time-dependent discharge curve of a 4.4 mF energy storage capacitor, which is approximately 0.1 mJ/s and 0.015 mJ/s, respectively (Fig. S14). Fig. 4d displays the ambient temperature and humidity data profiles collected continuously from the wireless sensor for 10 weeks. It suggests that the proposed VI-MME harvester supplies adequate power to continuously drive the wireless sensor systems for longer times without any communication interruption.

Further, we utilize the low-amplitude stray magnetic fields generated from the power lines of home appliances to demonstrate the VI-MME harvester as a sustainable power source for driving real-life IoT-based wireless applications, as schematically presented in Fig. 5a. The power cables of home appliances can produce 50/60 Hz magnetic fields up to several Oe, and these magnetic fields can be harvested and used for the condition monitoring of various home appliances. Therefore, we installed the VI-MME harvester inside a specially designed module/chamber near the power cable of an air conditioner (video S1), and then, the harvested energy is rectified *via* an LTC 3588 energy conversion circuit and supplied to an IoT temperature and humidity sensor, as shown in Fig. 5b. The estimated magnetic field inside the chamber containing a power cable of the air conditioner in the working/ON condition (with a set of temperature of 22 °C) is approximately 2.2 Oe (Fig. S15). The VI-MME harvester generated a 60 Hz root mean square (RMS) power of 10.6 mW under the stray magnetic field of 2.2 Oe, which is almost similar to the output power generated by using the Helmholtz coil (12.2 mW at 2.5 Oe). This means that the VI-MME harvester can generate high output power even in the realistic conditions without any significant degradation. The "no signal" image in Fig. 5c-i represents the disconnected state of the sensor or switch off state of the air conditioner. When the air conditioner is turned on, the VI-MME harvester quickly charges the energy storage capacitor up to 3.6 V. Then the charged capacitor supplies the power to operate the sensor and simultaneously send the temperature and humidity information to the smartphone, as seen in the real-time data display on the monitoring application of the smartphone in Fig. 5c-ii ("transferred data" image) and video S2. The averaged data profiles of the temperature and humidity information collected during the daytime for 10 weeks are displayed in Fig. 5d–i and ii. Further, the sensitivity and detection limits of the self-powered wireless sensor system to the stray magnetic fields were provided in Figs. S16-S18. The above demonstrations prove that the utilization of the vertical installation and heavy magnetic proof mass enhances the output performance of the MME harvester in terms of output power and lifetime, providing a sustainable power source to operate real-life IoT applications.

Supplementary material related to this article can be found online at doi:10.1016/j.nanoen.2022.107567.

4. Conclusions

A highly sustainable MME energy harvester with enhanced output performance is demonstrated by applying the vertical configuration of a cantilever with a heavy magnetic proof mass. The adoption of the heavier magnetic proof mass facilitated the amplification of magneto-mechanical bending vibration in a low magnetic field, while the vertical installation extended the lifetime of the MME harvester by reducing the gravity-induced bending effect on the cantilever structure. The VI-MME harvester generated a maximum output power of 12.2 mW under a magnetic field of 2.5 Oe, which is much larger than that of previously reported ME coupled MME harvesters. The ALT method is utilized to predict the lifetime of the VI-MME harvester under the normal use condition (~2.5 Oe) by establishing a relation between the lifetime and different stress levels of 2000, 2500, 3000 με using the IPL-Weibull model. The estimated usable lifetime of the VI-MME harvester with a 62.3 % failure probability is approximately 2.5×10^9 cycles. The practicability of the VI-MME harvester is confirmed by continuously operating the environmental (temperature and humidity) sensors and wireless data communication systems for 10 weeks by harvesting the 60 Hz stray magnetic fields of below 2.2 Oe. The obtained results provide a new approach to enhance the power efficiency and longevity of the MME harvesters.

CRediT authorship contribution statement

Min Sub Kwak: Experiment, Writing-original draft. **Mahesh Peddigari:** Experiment, Writing-original draft. **Yuho Min**: Conceptualization, Investigation, Writing-review & editing. **Jong-Jin Choi**: Conceptualization, Investigation, Writing-review & editing. **Jong-Hyun Kim**: Conceptualization, Investigation, Writing-review & editing. **Michael Abraham Listyawan**: Conceptualization, Investigation, Writing-review & editing. **Jungho Ryu**: Conceptualization, Investigation, Writing-review & editing. **Geon-Tae Hwang**: Conceptualization, Investigation, Writing-review & editing. **Woon-Ha Yoon**: Conceptualization, Investigation, Writing-review & editing. **Jongmoon Jang**: Supervision, Investigation, Writing-review & editing.

Declaration of Competing Interest

The authors declare that they have no known competing interests.

Data availability

Data will be made available on request.

Acknowledgments

This work is funded by a Korea Institute of Materials Science (PNK8240), a National Research Council of Science & Technology (NST) grant by the Korean government (MSIP) (No. CAP-17–04-KRISS), and a National Research Foundation of Korea (NRF) grant funded by the Korean government (MSIT) (No. 2020R1F1A107422211), and a Korea Medical Device Development Fund grant funded by the Korea Government (No. KMDF_PR_20210527_0007–2021-02).

Appendix A. Supporting information

Supplementary data associated with this article can be found in the online version at doi:10.1016/j.nanoen.2022.107567.

References

[1] J. Gubbi, R. Buyya, S. Marusic, M. Palaniswami, Internet of Things (IoT): a vision, architectural elements, and future directions, Future Gen. Comp. Syst. 29 (2013) 1645–1660.
[2] J.M. Perkel, The Internet of Things comes to the lab, Nature 542 (2017) 125–126.
[3] C. Lethien, J. Le Bideau, T. Brousse, Challenges and prospects of 3D micro-supercapacitors for powering the internet of things, Energy Environ. Sci. 12 (2019) 96–115.
[4] M. Feng, Y. Wu, Y. Feng, Y. Dong, Y. Liu, J. Peng, N. Wang, S. Xu, D. Wang, Highly wearable, machine-washable, and self-cleaning fabric-based triboelectric nanogenerator for wireless drowning sensor, Nano Energy 93 (2022), 106835.
[5] Y. Feng, E. Benassi, L. Zhang, X. Li, D. Wang, F. Zhou, W. Liu, Concealed wireless warning sensor based on triboelectrification and human-plant interactive induction, Research 2021 (2021), 9870936.
[6] Y. Feng, Y. Dong, L. Zhang, X. Li, L. Li, Y. Zheng, D. Wang, F. Zhou, W. Liu, Green plant-based triboelectricity system for green energy harvesting and contact warning, EcoMat 3 (2021), e12145.
[7] C.R. Bowen, H.A. Kim, P.M. Weaver, S. Dunn, Piezoelectric and ferroelectric materials and structures for energy harvesting applications, Energy Environ. Sci. 7 (2014) 25–44.
[8] M. Peddigari, M.S. Kwak, Y. Min, C.-W. Ahn, J.-J. Choi, B.D. Hahn, C. Choi, G.-T. Hwang, W.-H. Yoon, J. Jang, Lifetime estimation of single crystal macro-fiber composite-based piezoelectric energy harvesters using accelerated life testing, Nano Energy 88 (2021), 106279.
[9] Z.L. Wang, J. Chen, L. Lin, Progress in triboelectric nanogenerators as a new energy technology and self-powered sensors, Energy Environ. Sci. 8 (2015) 2250–2282.
[10] L.E. Bell, Cooling, heating, generating power, and recovering waste heat with thermoelectric systems, Science 321 (2008) 1457–1461.
[11] C.R. Bowen, J. Taylor, E. LeBoulbar, D. Zabek, A. Chauhan, R. Vaish, Pyroelectric materials and devices for energy harvesting applications, Energy Environ. Sci. 7 (2014) 3836–3856.
[12] S. Yun, Y. Qin, A.R. Uhl, N. Vlachopoulos, M. Yin, D. Li, X. Han, A. Hagfeldt, New-generation integrated devices based on dye-sensitized and perovskite solar cells, Energy Environ. Sci. 11 (2018) 476–526.
[13] B.E. Hardin, E.T. Hoke, P.B. Armstrong, J.-H. Yum, P. Comte, T. Torres, J.M. J. Fréchet, M.K. Nazeeruddin, M. Grätzel, M.D. McGehee, Increased light harvesting in dye-sensitized solar cells with energy relay dyes, Nat. Photon. 3 (2009) 406–411.
[14] G. Liu, P. Ci, S. Dong, Energy harvesting from ambient low-frequency magnetic field using magneto-mechano-electric composite cantilever, Appl. Phys. Lett. 104 (2014), 032908.
[15] V. Annapureddy, S.-M. Na, G.-T. Hwang, M.G. Kang, R. Sriramdas, H. Palneedi, W.-H. Yoon, B.-D. Hahn, J.-W. Kim, C.-W. Ahn, D.-S. Park, J.-J. Choi, D.-Y. Jeong, A. B. Flatau, M. Peddigari, S. Priya, K.-H. Kim, J. Ryu, Exceeding milli-watt powering magneto-mechano-electric generator for standalone-powered electronics, Energy Environ. Sci. 11 (2018) 818–829.
[16] K.-W. Lim, M. Peddigari, C.H. Park, H.Y. Lee, Y. Min, J.-W. Kim, C.-W. Ahn, J.-J. Choi, B.-D. Hahn, J.-H. Choi, D.-S. Park, J.-K. Hong, J.-T. Yeom, W.-H. Yoon, J. Ryu, S.N. Yi, G.-T. Hwang, A high output magneto-mechano-triboelectric generator enabled by accelerated water-soluble nano-bullets for powering a wireless indoor positioning system, Energy Environ. Sci. 12 (2019) 666–674.
[17] M.G. Kang, R. Sriramdas, H. Lee, J. Chun, D. Maurya, G.T. Hwang, J. Ryu, S. Priya, High power magnetic field energy harvesting through amplified magneto-mechanical vibration, Adv. Energy Mater. 8 (2018), 1703313.
[18] H. Song, D.R. Patil, W.-H. Yoon, K.-H. Kim, C. Choi, J.-H. Kim, G.-T. Hwang, D.-Y. Jeong, J. Ryu, Significant power enhancement of magneto-mechano-electric generators by magnetic flux concentration, Energy Environ. Sci. 13 (2020) 4238–4248.
[19] H. Lee, R. Sriramdas, P. Kumar, M. Sanghadasa, M.G. Kang, S. Priya, Maximizing power generation from ambient stray magnetic fields around smart infrastructures enabling self-powered wireless devices, Energy Environ. Sci. 13 (2020) 1462–1472.
[20] V. Annapureddy, M. Kim, H. Palneedi, H.-Y. Lee, S.-Y. Choi, W.-H. Yoon, D.-S. Park, J.-J. Choi, B.-D. Hahn, C.-W. Ahn, J.-W. Kim, D.-Y. Jeong, J. Ryu, Low-loss piezoelectric single-crystal fibers for enhanced magnetic energy harvesting with magnetoelectric composite, Adv. Energy Mater. 6 (2016), 1601244.
[21] G. Liu, X. Li, J. Chen, H. Shi, W. Xiao, S. Dong, Colossal low-frequency resonant magnetomechanical and magnetoelectric effects in a three-phase ferromagnetic/elastic/piezoelectric composite, Appl. Phys. Lett. 101 (2012), 142904.
[22] J. Ryu, J.-E. Kang, Y. Zhou, S.-Y. Choi, W.-H. Yoon, D.-S. Park, J.-J. Choi, B.-D. Hahn, C.-W. Ahn, J.-W. Kim, Y.-D. Kim, S. Priya, S.Y. Lee, S. Jeong, D.-Y. Jeong, Ubiquitous magneto-mechano-electric generator, Energy Environ. Sci. 8 (2015) 2402–2408.
[23] R. Sriramdas, M.-G. Kang, M. Meng, M. Kiani, J. Ryu, M. Sanghadasa, S. Priya, Large power amplification in magneto-mechano-electric harvesters through distributed forcing, Adv. Energy Mater. 10 (2020), 1903689.
[24] V. Annapureddy, H. Palneedi, G.-T. Hwang, M. Peddigari, D.-Y. Jeong, W.-H. Yoon, K.-H. Kim, J. Ryu, Magnetic energy harvesting with magnetoelectrics: an emerging technology for self-powered autonomous systems, Sust. Energy Fuels 1 (2017) 2039–2052.
[25] S. Dong, J. Zhai, J.F. Li, D. Viehland, S. Priya, Multimodal system for harvesting magnetic and mechanical energy, Appl. Phys. Lett. 93 (2008), 103511.
[26] D.Y. Hyeon, C. Nam, S.S. Ham, G.-T. Hwang, S. Yi, K.T. Kim, K.-I. Park, Energy harvesting: enhanced energy conversion performance of a magneto–mechano–electric generator using a laminate composite made of piezoelectric polymer and metallic glass (Adv. Electron. Mater. 1/2021), Adv. Electron. Mater. 7 (2021), 2170002.
[27] G.-Y. Kim, M. Peddigari, K.-W. Lim, G.-T. Hwang, W.-H. Yoon, H. Choi, J.W. Lee, J. Ryu, Effect of thickness ratio in piezoelectric/elastic cantilever structure on the piezoelectric energy harvesting performance, Electron. Mater. Lett. 15 (2019) 61–69.
[28] M. Peddigari, K.-W. Lim, M. Kim, C.H. Park, W.-H. Yoon, G.-T. Hwang, J. Ryu, Effect of elastic modulus of cantilever beam on the performance of unimorph type piezoelectric energy harvester, APL Mater. 6 (2018), 121107.
[29] A. Thakre, A. Kumar, D.-Y. Jeong, G.-T. Hwang, W.-H. Yoon, H.-Y. Lee, J. Ryu, Enhanced mechanical quality factor of 32 mode Mn doped 71Pb(Mg1/3Nb2/3)O3–29PbZrTiO3 piezoelectric single crystals, Electron. Mater. Lett. 16 (2020) 156–163.
[30] M.S. Kwak, M. Peddigari, H.Y. Lee, Y. Min, K.-I. Park, J.-H. Kim, W.-H. Yoon, J. Ryu, S.N. Yi, J. Jang, G.-T. Hwang, Exceeding 50 mW RMS-output magneto-mechano-electric generator by hybridizing piezoelectric and electromagnetic induction effects, Adv. Funct. Mater. 32 (2022) 2112028.
[31] M. Shirvanimoghaddam, K. Shirvanimoghaddam, M.M. Abolhasani, M. Farhangi, V.Z. Barsari, H. Liu, M. Dohler, M. Naebe, Towards a green and self-powered internet of things using piezoelectric energy harvesting, IEEE Access 7 (2019) 94533–94556.
[32] S. Limon, O.P. Yadav, H. Liao, A literature review on planning and analysis of accelerated testing for reliability assessment, Qual. Rel. Eng. Int. 33 (2017) 2361–2383.
[33] Internaltional Standard Methods for product accelerated testing (IEC 62506), The International Electrotechnical Commission (IEC), 2013.
[34] R. Salazar, M. Serrano, A. Abdelkefi, Fatigue in piezoelectric ceramic vibrational energy harvesting: a review, Appl. Energy 270 (2020), 115161.
[35] N. Núñez, J.R. González, M. Vázquez, C. Algora, P. Espinet, Evaluation of the reliability of high concentrator GaAs solar cells by means of temperature accelerated aging tests, Prog. Photovolt. Res. Appl. 21 (2013) 1104–1113.
[36] B.M. Mogilevsky, G.A. Shirn, Accelerated life tests of ceramic capacitors, IEEE Trans. Comp. Hybrids Manfact. Technol. 11 (1988) 351–357.
[37] P. Espinet-González, C. Algora, N. Núñez, V. Orlando, M. Vázquez, J. Bautista, K. Araki, Temperature accelerated life test on commercial concentrator III–V triple-junction solar cells and reliability analysis as a function of the operating temperature, Prog. Photovolt. Res. Appl. 23 (2015) 559–569.
[38] P.D.T. O'Connor, A. Kleyner. Practical Reliability Engineering, Fifth Edition, Wiley, 2011.
[39] D. Galar, U. Kumar, Prognosis. eMaintence, Academic Press,, 2017, pp. 341–343.
[40] J. Chen, E. Zio, J. Li, Z. Zeng, C. Bu, Accelerated life test for reliability evaluation of pneumatic cylinders, IEEE Access 6 (2018) 75062–75075.

Mr. Min Sub Kwak is currently a researcher in the Korea Institute of Materials Science (KIMS), and he is pursuing his M. S. degree at the Korea Maritime and Ocean University. He graduated from Korea Maritime and Ocean University with his B.S. degrees in major of Electronic Material Engineering. His research interests focus on the energy harvesting technologies, piezoelectric and triboelectric energy.

Dr. Mahesh Peddigari is currently working as an assistant professor in the Department of Physics, IIT Hyderabad (IITH). He received his B.Sc and M.Sc degrees from Kakatiya University and Ph.D. degree from IIT Guwahati. Prior to joining at IITH, he was a post-doctoral fellow (2017–2022) at the Department of Functional Ceramics, Korea Institute of Materials Science (KIMS), South Korea. His research interests are in the fields of Relaxor ferroelectrics, Magnetoelectrics, Energy harvesting, and Multifunctional ceramic thin/thick films.

Dr. Woon-Ha Yoon is Principal Researcher at Korea Institute of Materials Science (KIMS), South Korea in Department of Functional Ceramics. He received his B.S. and M.S. degrees from the Inha University in 1989 and 1992, respectively, both of them in the field of Applied Physics. Since then, he was senior researcher at Korea Institute of Machinery & Materials (KIMM) (1992–1996). He received his Ph.D. degree in the Physics from Pukyong National University in 2001, His current research interests include Design of high-power ultrasound system, Design/Simulation of Piezoelectric MEMS devices and Thermoelectric/piezoelectric energy harvesters.

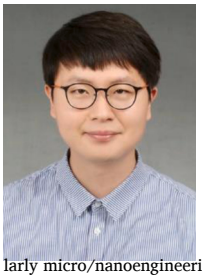

Dr. Jongmoon Jang is a Senior researcher of Department of Functional Ceramics at Korea Institute of Materials Science (KIMS) since 2019. He received his Ph.D. degree in the Department of Robotics Engineering from Daegu Gyeongbuk Institute of Science and Technology (DGIST) in 2017. He was postdoctoral fellow of Microsystems Laboratory at the École polytechnique fédérale de Lausanne (EPFL), Switzerland (2017–2019). His main research focuses on the development and reliability evaluation of piezoelectric devices such as vibrational/magneto-mechano-electric energy harvesters, acoustic sensors, and actuators. In parallel, he works on various aspects of microelectromechanical System (MEMS) particularly micro/nanoengineering in biomedical applications (BioMEMS) and carbon/ceramic materials (C-MEMS).